ELSEVIER

Chemical Geology 237 (2007) 433–449

CHEMICAL GEOLOGY
INCLUDING
ISOTOPE GEOSCIENCE

www.elsevier.com/locate/chemgeo

Immiscibility between carbonic fluids and granitic melts during crustal anatexis: A fluid and melt inclusion study in the enclaves of the Neogene Volcanic Province of SE Spain

B. Cesare [a,b,*], C. Maineri [a], A. Baron Toaldo [c], D. Pedron [c], A. Acosta Vigil [b]

[a] *Department of Mineralogy and Petrology, University of Padova, Corso Garibaldi, 37, I-35137 Padova, Italy*
[b] *Istituto di Geoscienze e Georisorse, CNR, Corso Garibaldi, 37, I-35131 Padova, Italy*
[c] *Department of Chemical Sciences, University of Padova, Via Marzolo, 1, I-35131 Padova, Italy*

Accepted 20 July 2006

Editor: R.L. Rudnick

Abstract

In the restitic crustal enclaves in the Neogene volcanics of El Hoyazo and Mazarrón (SE Spain), associations of fluid and silicate melt inclusions indicative of immiscibility are frequently observed in the Bt-poor, Crd-rich graphitic metapelites. These occurrences, extremely rare for anatectic crustal rocks, have been studied by microthermometry, micro-Raman spectroscopy and EMP analysis. Both at El Hoyazo and Mazarrón the immiscible FI and MI are hosted in plagioclase and cordierite, with microstructures that suggest primary trapping. The FI hosted in cordierite are monophase, whereas they may contain crystals of calcite when hosted in plagioclase, indicating fluid–host reaction during cooling. Decrepitation microstructures have not been observed. The MI contain fresh glass of peraluminous, felsic rhyolitic composition, typical of anatectic S-type melts. In all samples the fluids are CO_2-dominated (>85 mol%), with minor amounts of N_2 and CH_4, and traces of CO and H_2. The nucleation of graphite, induced by the laser beam in some inclusions, demonstrates that the fluids are graphite-saturated. Large scatter in microthermometric behaviour of FI indicates significant density variations. Only in one sample from El Hoyazo are fluid densities compatible with the estimated *P–T* conditions of trapping (5–7 kbar, 850±50 °C), whereas in the remaining samples the extremely low densities, suggesting trapping pressures <1 kbar, are in contrast with the microstructural indications of primary entrapment and little evidence of decrepitation. In addition, although some measured compositions are compatible with C–O–H–N fluid speciation at the estimated *P–T* conditions of anatexis, the lack of H_2O in all FI is inconsistent with the slightly hydrated character of coexisting glasses. The possible mechanisms accounting for departure of densities and compositions of FI from expected values are discussed, and leakage of H_2O suggested as the most plausible.

Keywords: Anatexis; CO_2; Cordierite; Fluid inclusions; Graphite; Melt inclusions

1. Introduction

The interactions and equilibria between melt, fluid, and solid phases are critical parameters for understanding the processes operating in the lower crust and upper mantle, main loci of generation of magmas. In turn,

* Corresponding author. Department of Mineralogy and Petrology, University of Padova, Corso Garibaldi, 37, I-35137 Padova, Italy. Fax: +39 049 827 2010.
E-mail address: bernardo.cesare@unipd.it (B. Cesare).

0009-2541/$ - see front matter © 2006 Elsevier B.V. All rights reserved.
doi:10.1016/j.chemgeo.2006.07.013

these relationships are also critical in governing magma segregation and migration, and the differentiation of the lithosphere and its rheology.

Experimental studies (e.g., Holloway, 1976; Tamic et al., 2001) have shown that compared with H_2O, carbonic fluids have a very low solubility in silicate melts and, therefore, there is the potential for CO_2-rich fluids to separate as an independent phase from the CO_2-saturated magma, giving rise to the phenomenon of *immiscibility*. Fluid-melt immiscibility is well known and extensively studied through fluid inclusions (Roedder and Coombs, 1967; Roedder, 1992). Immiscibility between mafic melts and CO_2-rich fluids is commonly found in natural mafic systems (e.g. in mantle xenoliths and basalt xenocrysts or phenocrysts; Roedder, 1965; Andersen and Neumann, 2001), and is much more rarely reported from silicic melts (e.g., Roedder and Coombs, 1967; De Vivo and Frezzotti, 1994; Frezzotti et al., 1994). Immiscibility is generally associated with two processes occurring *after* magma generation: one is the differentiation by crystal fractionation, discussed in detail by Roedder (1992); the other is magma uprise and outgassing. In both cases, as the primary features (and the volatile contents) of the magma at the time of formation have been modified by either cooling and/or decompression, the immiscible melt and fluid, trapped by crystallizing minerals are "*almost always nonrepresentative of the bulk of the magma*" (Roedder, 1992).

A different scenario is when immiscibility is a *primary* feature attained at the moment of magma generation, for example during partial melting in the presence of a fluid (e.g., CO_2) of limited solubility in the anatectic melt. In this case, the growing peritectic minerals could be able to trap these immiscible fluids as coexisting melt (MI) and fluid inclusions (FI). When the attention is focussed on crustal anatexis and origin of S-type granites, it can be observed that although carbonic fluids are frequently detected in felsic granulites and anatectic migmatites (e.g., Touret, 1971, 1981), fluid-melt immiscibility is seldom described as a primary feature. This is probably due to the slow cooling and recrystallization of high-grade metamorphic rocks, which make preservation of FI and MI unlikely. Therefore, witness of this type of primary immiscibility should be preferentially sought in rapidly cooled xenoliths, even though most occurrences (summarized by Lowenstern, 1995) pertain to mafic magma systems.

This paper reports on an exceptional natural example of primary immiscibility between crustal anatectic granitic melts and carbonic fluids, characterized in residual, partially melted enclaves from the volcanics of SE Spain. The preservation of FI and MI coexisting in plagioclase and cordierite have allowed their chemical characterization, discussion of post-entrapment modifications of inclusions, and evaluation of the implications for the role of fluids during crustal anatexis in this particular geodynamic scenario.

2. Geological setting and sample petrography

The crustal enclaves in the intermediate to felsic volcanics of the Neogene Volcanic Province (NVP) of SE Spain represent partially melted fragments of metapelite which, after anatexis and melt extraction, were rapidly uprisen and cooled through eruption in a submarine environment (Zeck, 1970; Cesare et al., 1997; Álvarez-Valero, 2004). The fast cooling has allowed preservation of mineralogical, textural and geochemical features of partially melted systems, as testified by the occurrence in the enclaves of fresh, undevitrified silicate glass (former melt).

The residual enclaves studied in this paper, collected from the outcrops of El Hoyazo and Mazarrón (Fig. 1), have been the subject of detailed studies in the last decade (Cesare et al., 2003a; Álvarez-Valero et al., 2005, and references therein). These rocks are thought to represent fragments of the thinned lower continental crust of the Internal Betics, lying above hot asthenospheric mantle, whose anatexis, fragmentation and emplacement gave rise to "erupted migmatites" as in the definition of Zeck (1970). The *P–T* conditions and ages of partial melting have been estimated at c. 850 °C and 5–7 kbar at 9.6 Ma for El Hoyazo, and 850±50 °C and c. 4 kbar at 9.1 Ma for Mazarrón (Cesare et al., 1997; Cesare et al., 2003a; Álvarez-Valero, 2004). Therefore the two outcrops testify for slightly different depths of melting in the crust. This is supported by the mineral assemblages of the enclaves, dominated by garnet at El Hoyazo and by cordierite at Mazarrón.

A peculiar characteristic of most crustal enclaves of the NVP is the abundance of inclusions of glass (hereafter melt inclusions, MI) in most mineral phases (Cesare et al., 1997; Cesare et al., 2003b; Álvarez-Valero et al., 2005). The arrangement of MI indicates a primary origin, i.e. the entrapment during the growth of the host (Cesare et al., 1997; Álvarez-Valero et al., 2005; Acosta-Vigil et al., 2007-this issue). As the enclaves represent partially melted, residual metapelites, we interpret these primary melt inclusions as the silicate liquid trapped during peritectic melting reactions in which solids and melt were generated simultaneously. The lack of interaction between enclaves and their host lava, and the lack of impregnation of enclaves by external melts have been discussed elsewhere (Cesare

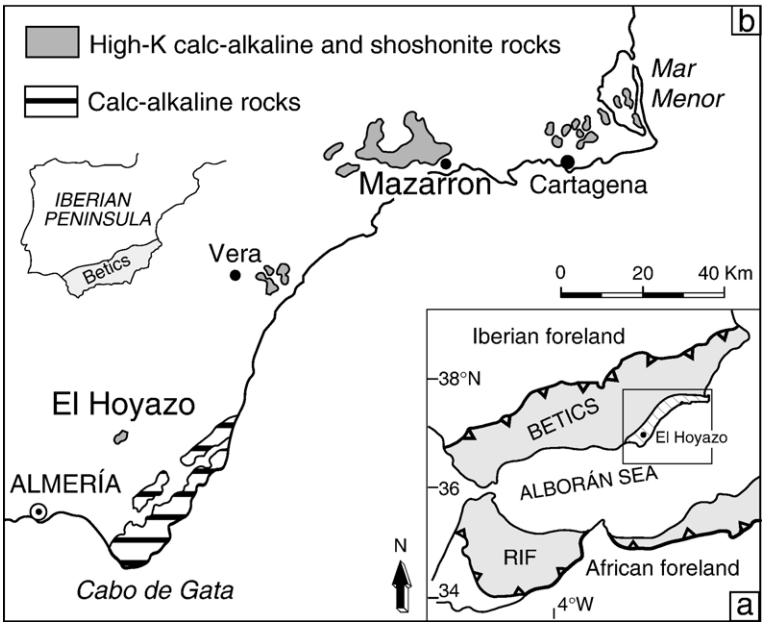

Fig. 1. The Neogene Volcanic Province of SE Spain. a) Geographic location and schematic tectonic elements of the Alborán domain; box indicates area enlarged in (b) and diagonal pattern the Volcanic Province. b) The main outcrops of the Neogene Volcanic Province.

et al., 1997; Cesare and Gomez-Pugnaire, 2001) and attest that the enclaves do not represent rock fragments which melted or re-melted by interaction with the lava during entrainment or transport. Conversely, they belong to a crystalline basement, which melted during deformation, was fragmented and entrained in the anatectic melt with which it was in thermal equilibrium, and finally was brought to the surface by volcanic eruption. Unlike what is often the case for sedimentary xenoliths, the enclaves were not re-heated during transport to the surface, the major changes undergone being sudden decompression, followed by fast cooling.

Unlike MI, FI are very rare in the enclaves of the NVP. Cesare and Maineri (1999) noted that they do not occur in the most common enclave type (Bt–Grt–Sil) of El Hoyazo, even though the melting process was probably fluid-present. The rare samples from El Hoyazo where FI have been found are Crd-bearing, Bt-poor rocks (mineral abbreviations after Kretz, 1983, Gl = glass), and the same is observed at Mazarrón.

The FI-bearing samples are medium-grained hornfelses characterised by the mineral assemblage Crd–Sil–Pl–Gl–Ilm–Gr ± Bt ± Grt ± Spl ± Qtz ± Kfs ± And. Biotite is rare to absent; garnet may occur as resorbed relicts, replaced by cordierite; hercynite is a common phase in equilibrium with cordierite; quartz and K-feldspar are mutually exclusive; andalusite is a metastable relict in the samples from Mazarrón. Overall, these rocks share most petrographic features of sample AV-HZ8, studied here and described in detail also by Cesare et al. (2005).

FI have been found within plagioclase and cordierite host crystals, and are frequently associated with MI in microstructures that indicate immiscibility between two coexisting "fluid" phases. Such extremely rare occurrences for crustal rocks are the subject of the following description, data and discussion, which only refer, unless explicitly stated, to FI and MI that are interpreted from their microstructural features as having been trapped simultaneously.

3. Samples and methods

Several normal thin sections, polished thin sections and doubly polished thick (c. 100 μm) sections from three crustal enclaves (samples AVHZ7 and AVHZ8 from El Hoyazo, and AVMA7 from Mazarrón) were used for petrographic, microthermometric, laser Raman micro spectroscopy and electron microprobe (EMP) analyses of FI and MI.

Microthermometry was carried out at the Department of Mineralogy and Petrology of Padova University. About 200 fluid inclusions representative of the various populations were analyzed by means of a Linkam TH600 heating–freezing stage, adapted on a Zeiss transmitted light optical microscope. Accuracy was ±0.2 °C in the

−100/+31 °C temperature range. Phase transitions at $T<32$ °C were observed at a heating rate of 0.5 °C/min. Instrument calibration was done by using synthetic pure CO_2 and pure H_2O fluid inclusion standards.

Raman analyses were carried out at the Department of Chemical Sciences of Padova University using a home made micro-Raman system, based on a single 320 mm focal length imaging spectrograph (Triax-320 Jobin Yvon), equipped with a holographic 1800 g/mm grating and a liquid nitrogen cooled CCD detector. The excitation source was a Spectra Physics Ar^+ ion laser (mod. Stabilite 2017) operating at 488 and 514.5 nm, appropriate holographic notch filters were used to reduce the stray-light level. An optical microscope (Olimpus BX 40) equipped with three objectives, 20×/0.35, 50×/0.75 and 100×/0.90, was optically coupled to the spectrograph and used to record the Raman spectra in micro configuration. In the present work all Raman analyses (qualitative and quantitative) have been performed by using the 514.5 nm line as exciting radiation, and only in a few cases – to avoid fluorescence effects from the sample – by the 488 nm line. The irradiation power on the sample was typically 25–30 mW. The Raman spectra were recorded between 250 and 4300 cm^{-1} with an instrumental resolution of about 2 cm^{-1}; integration times were typically of 10–30 s. The molar ratios of components in fluid inclusions, χ_a, were calculated using the following relation:

$$\chi_a = [A_a/(\sigma_a\zeta_a)]/\Sigma_i[A_i/(\sigma_i\zeta_i)]$$

where A_a is the area of the characteristic Raman scattering band of the component a, σ_a the Raman scattering cross section (Burke, 2001) and ζ_a the instrumental correction factor. Instrumental correction factors were estimated by using standard calibration Raman scattering data of cyclohexane (McCreery, 2000).

Silicate glass inclusions and their host minerals were analyzed with a Cameca SX-50 electron microprobe at the University of Oklahoma. Matrix reduction used the PAP correction algorithm (Pouchou and Pichoir, 1985). Analyses of MI were conducted using two analytical conditions as recommended by Morgan and London (1996). Na, K, Al and Si were analyzed using an accelerating voltage of 20 kV, 2 nA current, and a 5 μm beam diameter. The elements Fe, Mn, Mg, Ti, Ca, P, F and Cl were analyzed with a 20-kV, 20-nA, 5-μm beam. Na, Al and K were analyzed first and concurrently to minimize alkali loss and changes in major elemental ratios. Counting times were 30 s on peak for all elements, yielding 3σ minimum detection limits of ≈0.02 wt.% for Na_2O, K_2O and Al_2O_3, and ≈0.05 wt.% for SiO_2. Relative uncertainties based on counting statistics are in the range of 0.5–1.0% for Al_2O_3 and SiO_2, and 1.5–3.0% for Na_2O and K_2O. Analyses were corrected for small alkali loss using a hydrated metaluminous haplogranite glass secondary standard. The maximum uncertainty for reported ASI values is ±0.035, calculated by the propagation of errors. H_2O concentrations in glass were calculated by the difference of electron microprobe totals from 100%. Morgan and London (1996) and Acosta-Vigil et al. (2003) have shown that using the above methods, the accuracy of H_2O by difference is better than ±10% relative for H_2O concentrations in the range of 2–10 wt.%.

4. Fluid inclusion microstructures

Host minerals for the studied inclusions are cordierite and plagioclase in all samples from both localities, but it must be pointed out that FI are not homogenously distributed within the two localities and mineral phases: at El Hoyazo inclusions are much more abundant in cordierite than in plagioclase, while at Mazarrón the reverse is observed.

At room temperature, the majority of inclusions contains either a monophase low-density fluid (F), or a clear, fresh undevitrified glass (M) in which one shrinkage bubble can be observed. Also present are "mixed" F+M inclusions, where the glass phase may either occupy one side of the cavity or surround the gas

Fig. 2. Microstructures of FI and MI in the studied enclaves. a) Cluster of FI (F), MI (M) and "mixed" inclusions, with variable F/M proportions. The host also contains solid inclusions of graphite (Gr). Host: cordierite; locality: Mazarrón. b) Isolated, large MI. The shrinkage bubble does not contain any Raman-active species. Also present are secondary planes (S) of tubular FI. Host: cordierite; locality: El Hoyazo. c) Cluster of associated FI and MI, indicative of fluid immiscibility in a graphite-bearing rock. Host: cordierite; locality: El Hoyazo. d) Plagioclase crystal crowded with FI, MI and graphite inclusions. Inclusions are commonly located, with a patchy distribution, at the cores of the crystals. Arrows indicate the cleavage planes of plagioclase. Locality: Mazarrón. e) The relationships between these two large, asymmetric FI and the adjacent sillimanite needles (Sil, arrows) suggest that entrapment of FI was aided by sticking of fluid droplets to the sillimanite during growth of the host cordierite. Locality: El Hoyazo. f) Close up of Fig. 2d, showing the tendency of dark FI to form negative crystals with two planar faces parallel to the host's cleavage (black arrows). White arrows point to small solids within FI, determined as calcite by Raman analysis. Host: plagioclase; locality: Mazarrón. g) Cluster of spherical to ovoidal immiscible FI and MI. Host: cordierite; locality: El Hoyazo. h) Immiscible FI and MI showing elongation parallel to the *c* axis of the cordierite host. Arrows point to reentrants in the FI cavities, determined as cordierite by Raman analysis. Locality: Mazarrón. i) Rare occurrence of fluid (double meniscus) within the shrinkage bubble of a large MI in plagioclase. Black arrows point to the cleavage planes of the host; white arrows show two tails of the MI, suggesting either necking down, or decrepitation. Locality: Mazarrón.

bubble. In these mixed inclusions (see also Lowenstern, 2003) the two phases (F and M) are present in all proportions from pure F to pure M (Fig. 2a). As FI, MI and mixed inclusions occur intimately associated within the same cluster, they are likely to belong to the same fluid inclusion array (FIA; Goldstein and Reynolds, 1994) and, therefore, to have been trapped in a single event. Such a mode of occurrence, and the

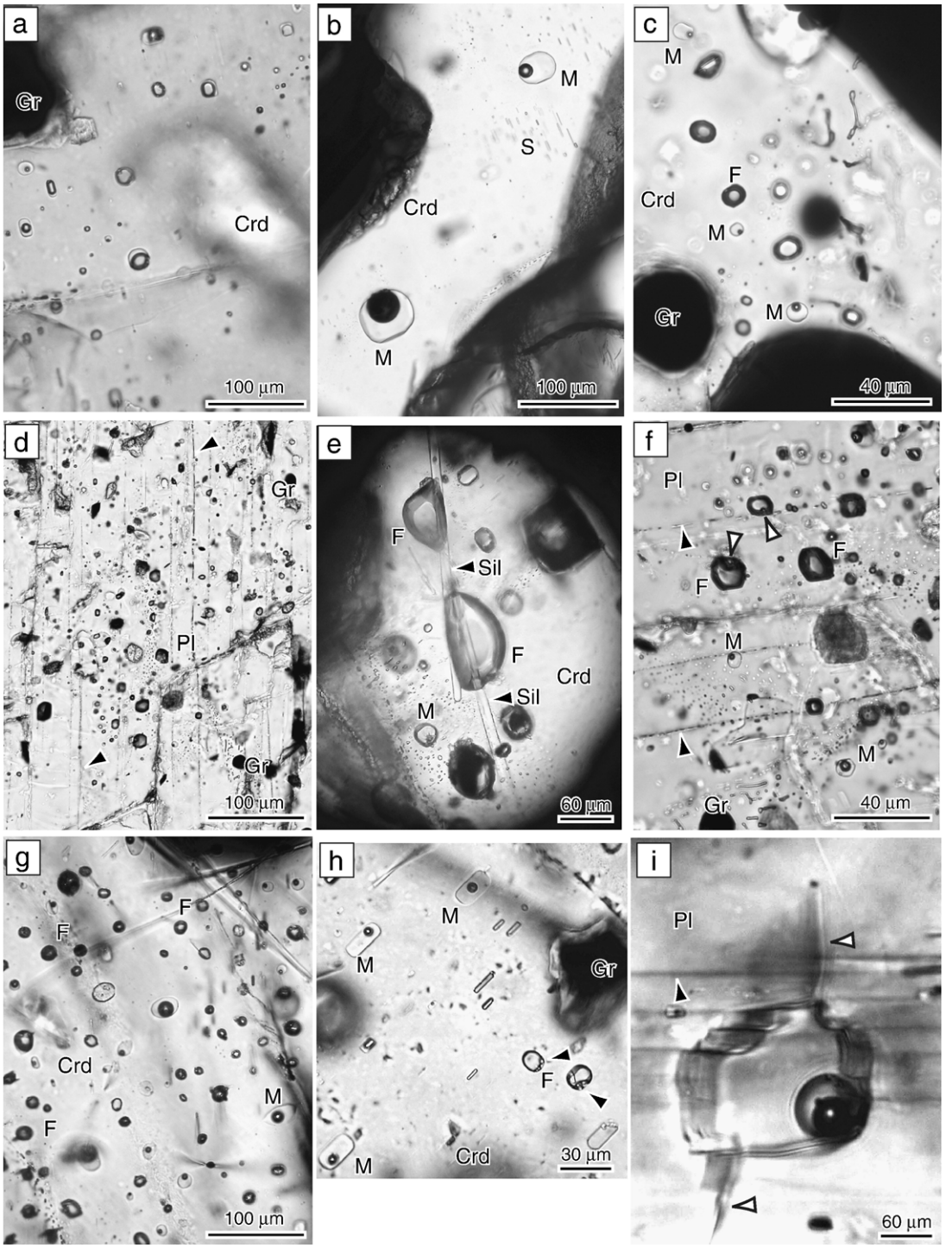

Table 1
EMP analyses of melt inclusions

Sample	AVHZ7	AVHZ8
No. analyses	51	5
SiO_2	73.56 (0.84)	71.98 (0.83)
TiO_2	0.07 (0.05)	0.08 (0.01)
Al_2O_3	14.07 (0.34)	13.33 (0.22)
FeO [a]	1.28 (0.13)	1.61 (0.11)
MnO	0.04 (0.04)	0.03 (0.01)
MgO	0.04 (0.07)	0.02 (0.02)
CaO	0.94 (0.15)	0.77 (0.06)
BaO	0.08 (0.05)	n.d.
Na_2O	3.41 (0.38)	3.35 (0.54)
K_2O	4.87 (0.59)	5.45 (0.42)
P_2O_5	0.20 (0.17)	0.21 (0.06)
F	0.05 (0.07)	0.03 (0.03)
Cl	0.45 (0.08)	0.44 (0.05)
O=F	−0.02 (0.03)	−0.01 (0.01)
O=Cl	−0.10 (0.02)	−0.10 (0.01)
H_2O by diff	0.95 (0.90)	2.81 (0.63)
#Mg	0.04 (0.06)	0.02 (0.02)
ASI	1.12 (0.04)	1.04 (0.024)
Norm Qtz	32.53	29.24
Norm Ab	28.85	28.35
Norm Or	28.78	32.21
Norm An	3.36	2.45
Norm Crn	1.96	1.02

[a] Total Fe as FeO.

variable *M* to *F* ratio within mixed inclusion, suggest that these FIA originated by simultaneous trapping of two immiscible phases, F and M.

Among the abundant inclusions of various origins, for this work we have considered primary or early trapped inclusions selected according to Roedder's (1984) microstructural criteria, i.e. either isolated (Fig. 2b) or small clusters (Fig. 2c) with respect to the crystallographic elements of host minerals. Primary origin is particularly evident in the case of most FIA hosted in plagioclase, which are commonly located at the core or in the inner portions of patchy zoned crystals (Fig. 2d). It is also evident by the spatial association of FI and MI with inclusions of fibrolite within cordierite (Fig. 2e), suggesting that, during cordierite growth, inclusion entrapment was facilitated by the presence of fibrolite needles on the surface of cordierite, to which fluid droplets would adhere. It follows that for the selected FIA the F/M immiscibility occurred during growth of the high-temperature anatectic Crd–Pl–Gl-bearing assemblage, i.e. early in the history of the rock and not during late, post-peak re-equilibration.

Plagioclases from Mazarrón host also several trails of workable pseudosecondary fluid inclusions outlining crystal twinning, and secondary fluid inclusions clearly related to a later fracturing event. Late fractures with FI are common also in cordierite. Pseudosecondary and secondary FIA, however, have been discarded for the current study.

Apparent diameters of the studied inclusions are in the range 5–30 μm, with rare isolated MI in cordierite reaching up to 100 μm. Both FI and MI may show negative crystal (Fig. 2f) or regular ovoidal to spherical morphologies (Fig. 2g), with frequent elongation along the *c* axis of Crd (Fig. 2h), or parallel to the cleavage planes of Pl. While there is evidence for the change in shape of inclusions via dissolution–precipitation processes at the cavity walls, which leads to necking down (Acosta-Vigil et al., 2007-this issue) and to the progressive development of negative crystal shapes, there are no microstructures pointing to post-trapping re-equilibration during decompression, such as shape irregularities or decrepitation halos around inclusions.

Peculiar features of Pl-hosted FI are their generally small size and the occurrence of a small rounded calcite crystal (Fig. 2f), that is interpreted as a mineral precipitated by chemical interactions between the fluid phase and the Ca-bearing host (Kleinefeld and Bakker, 2002). As far as cordierite concerns, the only solid rarely observed within FI is graphite; irregularities observed sometimes at the cavity walls and resembling daughter solids (Fig. 2h) consist also of cordierite.

The MI contain clear, colourless, isotropic and apparently homogenous glass with an empty shrinkage

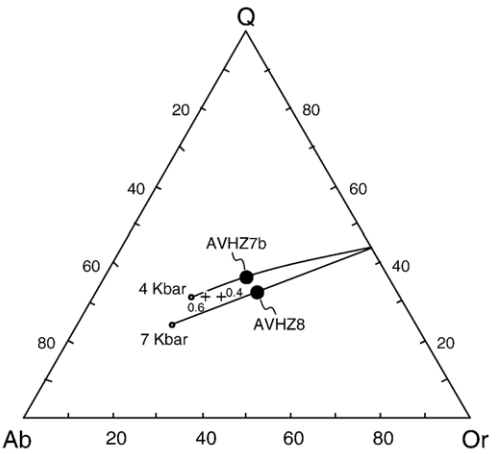

Fig. 3. Normative Qtz–Ab–Or composition (wt.%) of mean MI analyses (filled circles) in AVHZ-7b and AVHZ-8. Also shown are the cotectic lines for the H_2O-saturated granite system (projected from An) at 4 and 7 kbar, and the eutectic compositions for the haplogranite system at 4 and 7 kbar with $a_{H_2O}=1$ (black dots, taken from Winkler, 1974), and at 5 kbar with $a_{H_2O}=0.4$ and 0.6 (crosses, from Ebadi and Johannes, 1991).

bubble. Only rarely a double bubble has been observed, indicating the presence of fluid within MI (Fig. 2i). In the studied samples, there is no evidence of glass devitrification or weathering, or of crystallization of the melt as overgrowths at the inclusion walls.

5. Results

5.1. Electron microprobe analyses of melt inclusions and host minerals

Glass inclusions have been analyzed in cordierite from samples Av-Hz-7b and Av-Hz-8 (Table 1). The composition of glass in both samples is granitic and comparable, with high SiO_2 (72.0–73.5 wt.%) and low FeO_t (1.3–1.6 wt.%) and H_2O (≈0–3 wt.%) concentrations, extremely low MgO+TiO_2 (≈0.1 wt.%) and Mg numbers (0.02–0.04), and moderate to low ASI values (≈1.05–1.10). Fig. 3 shows that the mean analyses plot on the 4–7 kbar cotectic lines of the H_2O-saturated granite system in wt.% normative Q–Ab–Or (pseudo-ternary) space (Winkler, 1974), and toward the Q–Or sideline with respect to the 5-kbar haplogranite eutectic at $a_{H_2O}=0.4$ (Ebadi and Johannes, 1991). Compared with analyses of glass from dry partial melting experiments of metapelites at 800–900 °C and 7–10 kbar (e.g. Le Breton and Thompson, 1988; Vielzeuf and Holloway, 1988; Patiño Douce and Johnston, 1991), the current glass compositions are lower in H_2O, FeO_t and TiO_2 concentrations, and much lower in MgO concentration, Mg numbers and ASI values. Very low H_2O concentrations, considered as rare for MI in high-silica rhyolites (Lowenstern, 1995) strongly suggest melting at high temperature (>800 °C), H_2O-undersaturated conditions (e.g. Clemens and Vielzeuf, 1987; Johannes and Holtz, 1996). Low ASI values of liquids derived from strongly peraluminous protoliths can be explained, at least in part, by the extremely low H_2O concentrations in melt (Acosta-Vigil et al., 2003).

Cordierite has X_{Fe} 0.43–0.61 in samples from El Hoyazo, and 0.49–0.57 in samples from Mazarrón; plagioclase has X_{Fe} 0.50–63 in samples from El Hoyazo, and 0.40–0.48 in samples from Mazarrón.

5.2. Raman microspectroscopy

We investigated the spectral region from 1000 to 4300 cm^{-1}, where symmetrical vibration modes of most geologic gaseous components are known to occur. The spectra of Fig. 4 and the summary of Table 2 show that the fluid species detected within inclusions in both plagioclase and cordierite are CO_2, CH_4, N_2, CO and H_2, whereas H_2O is notably absent. Concerning fluid quantification, it is necessary to underline some specific features of cordierite. Due to its peculiar crystal structure, this mineral may accommodate in different positions within its structural channels various atomic and molecular species, mostly detected by IR- and/or mass spectroscopy. H_2O, CO_2 (e.g. Goldman et al., 1977; Aines and Rossman, 1984; Armbruster and Bloss, 1982), hydrocarbons, N_2 and noble gases, have long been known in natural cordierites, (e.g. Damon and Kulp, 1958; Mottana et al., 1983; Armbruster, 1985). Kolesov and Geiger (2000) precisely determined by means of Raman spectroscopy the nature and the allocation of H_2O and CO_2 channel constituents in several cordierite crystals from Ukraina, whereas Kalt (2000) reports the Raman detection of structural N_2 within cordierites from the German Variscides. It follows that during Raman detection and quantitative computations, the channel-filling molecules may interfere with volatiles contained within FI. We have therefore checked for the possible channel constituents also the cordierites from El Hoyazo and Mazarrón, in a number of randomly oriented samples. As a result, CO_2, CH_4, weak but clear CO and H_2 Raman bands, have been detected also within the same cordierites hosting fluid inclusions (Fig. 4). Alike within fluid inclusions, H_2O is basically absent, being detected only once, whereas CO_2 and CO appear to be common volatiles in all NVP cordierites. On the contrary, structural methane was only found at Mazarrón. As for N_2 in matrix channels, its occurrence cannot be ruled out in NVP cordierites, since a slight (~1 cm^{-1}) peak shift has been frequently observed with respect to N_2 inclusion bands (cf. Herms and Schenk, 1992). Although IR spectra of C–H stretching vibrations assigned to aliphatic hydrocarbons have been sometimes reported from cordierite (Mottana et al., 1983; Khomenko and Langer, 2000 and references therein) yet channel CH_4 has been reported only rarely, as in Kurepin et al. (1986). We are not aware of any finding of CO in cordierite channels, so that this appears as the first report.

Within cordierite, FI have been reported only rarely, and this mineral does not appear to be a common host for FI. Among recent studies, Herms and Schenk (1992) studied CO_2 (±N_2) FI hosted in cordierite from Calabrian granulitic metapelites, and Winslow et al. (1991) reported N_2-bearing inclusions from Massachusetts metapelites.

If Raman detection of structural fluids can be quite complex because of the strong influence of host crystal orientation on the allocation of molecular species in the channels, *quantification* of inclusion fluids in this host

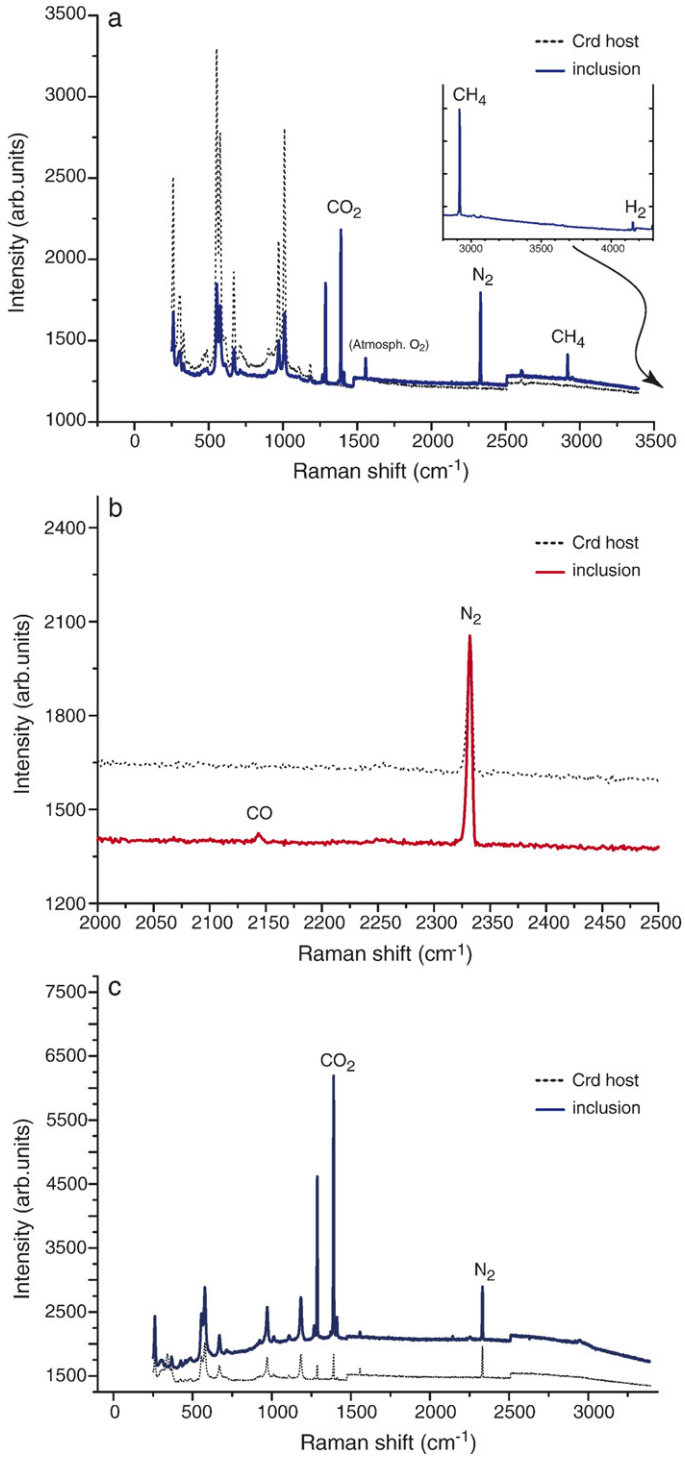

Fig. 4. Example of Raman spectra of CO_2–N_2–(CH_4–H_2) fluid inclusions and of matrix channel fluids from El Hoyazo cordierites (see text for operative conditions during acquisition).

is considered unreliable (Burke, 1994), owing to the mutual interference and superposition effects of Raman scattering from *structural* and *inclusion* fluids. In the present work, Raman spectra show very similar and consistent features over quite a large number (>100) of FI, and because of the agreement of estimated

Table 2
Composition (mol%) of representative fluid inclusions from the NVP xenoliths, calculated from Raman spectroscopy

Sample	FI host	CO_2	CH_4	N_2	CO	H_2	Solids
AVHZ7	Crd	80–96	0–3	3–16	0–9	0	Gr
	Pl	92–94	0	6–8	0	0	Cc
AVHZ8	Crd	86–97	0–1	0–11	0–2	0–1	Gr
	Pl	92–96	0	4–8	0	0–2	Cc
AVMA7	Crd	78–95	10–22	0–5	0–3	0	Gr
	Pl	90–100	2–10	0–5	0	0–3	Cc

compositions with microthermometric results, we infer that they can be taken as representative of the real fluid composition.

Finally, despite all uncertainties, due to the carbonic-dominated nature of FI, the possible errors on the quantification of gas molar fractions are expected to be minor and can be neglected when reconstructing the overall fluid nature and its volumetric properties.

The compositional ranges reported in Table 2 show that in samples from both localities CO_2 is by far the dominant phase, its relative molar fraction being always higher than 0.85 within Crd-hosted inclusions, and constantly >0.9 in Pl-hosted inclusions. Therefore, a first distinction between the Crd- and Pl-hosted fluids essentially relies in the nearly purity of the carbonic phase within these latter. More in detail, Raman analyses indicate that at Mazarrón the contaminant phase is CH_4 inside all inclusions (up to 22 mol%), rather than N_2 as in El Hoyazo fluids (up to 16 mol%). Additional species are CO (up to 9 mol%) and H_2 (up to 3 mol%), which are commonly detected in minor amounts in cordierite, but not in plagioclase. To sum up, we can describe fluids at El Hoyazo as CO_2–N_2 mixtures (±CO, H_2, CH_4), whereas fluids at Mazarrón as almost pure CO_2–CH_4 binaries. The composition of fluids is reported in the C–O–H projection of Fig. 5.

Concerning the solids observed within some Pl-hosted inclusions, all of them have been identified as calcite. The only other Raman signal detected is that of graphite, present in approximately 30% of Crd-hosted fluid inclusions from El Hoyazo samples. Graphite has also been observed to precipitate within inclusions during laser irradiation, indicating C-saturation of the fluids (e.g., van den Kerkhof et al., 1991). No graphite has been detected or precipitated in Pl-hosted inclusions.

In order to evaluate possible effects of species diffusion out of the inclusions, we have performed sample Raman profiles outside H_2-bearing fluid inclusions, both in plagioclase and in cordierite. Neither H_2, nor significant variations of volatile contents (i.e. CO_2 in cordierite) have been detected along these profiles.

5.3. Microthermometry

The microthermometric analyses were focussed on the low-density F inclusions, although during heating–cooling runs also some bubbles within "mixed" F+M were found to contain a gaseous carbonic phase with melting temperature at or below that of pure CO_2. These latter are not further considered here. Microthermometric results and estimated densities of measured FI are reported in Table 3.

On heating from −170 °C, the only observed phase transitions were melting of the CO_2 phase (T_{mCO_2}) and/or CO_2 homogenization (T_{hCO_2}). Although it should be expected that with the observed fluid compositions CO_2 melting occurs over a temperature interval (see van den Kerkhof and Thiery, 1994, 2001), allowing measurement of an initial melting temperature, the majority of inclusions was in most cases too dark to appreciate such phenomenon: on approaching T_{mCO_2}, only within a few inclusions could we see a modification of appearance that could be associated to the progress of a melting event. Neither ice nor clathrate were ever observed to form or to melt. As pointed out from data in Table 3, values of T_{mCO_2} are constantly lower than −56.6 °C and can reach −60 °C, in some Crd-hosted FI of El Hoyazo samples (Fig. 6). This indicates the presence of other species dissolved in the fluid, (as confirmed by Raman analyses). At El Hoyazo, besides CO_2, all Crd-hosted

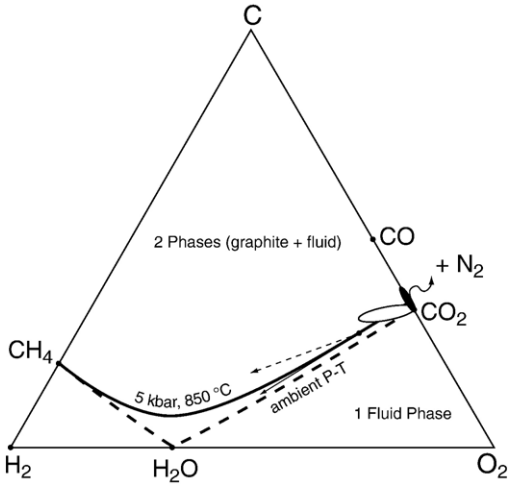

Fig. 5. C–O–H chemography reporting the composition of fluid inclusions determined in this study. White field: Mazarrón FI; black field: El Hoyazo FI (N_2 component considered graphically). Also reported are the carbon saturation surfaces for ambient P–T (dashed line) and for 5 kbar, 850 °C (solid line). Thin arrows pointing to H_2 (dashed) and H_2O (solid) help visualize the effect of leakage of these components (see text for details).

Table 3
Summary of microthermometric results from all studied inclusions

Sample	Microthermometry			Calculated properties	
	FI host and homog mode	T_{mCO_2} (°C)	T_{hCO_2} (°C)	Density range (g cm^{-3})	P range at 800–900 °C (kbar)
AVHZ7	Crd (liq)	−59.9/−56.8	5–24	0.73/0.82	3.6–4.0/2.2–2.5
	Crd (vap)	−59.9/−56.8	15–23	0.17/0.23	<0.5
	Pl (liq)	−57.9/−56.6	12–24	0.71/0.78	3.3–3.6/2.7–2.9
	Pl (vap)	−57.9/−56.6	17–23	0.18/0.23	<0.5
AVHZ8	Crd (vap)	−60.0/−56.8	18–24	0.19/0.23	<0.5
	Pl (vap)	−57.5/−56.6	15–23	0.17/0.23	<0.5
AVMA7P	Crd (vap)	−57.0/−59.5	15–23	0.18/0.20	<0.5
	Pl (vap)	−57.5/−56.6	14–25	0.18/0.23	<0.5

inclusions correctly show N_2 as the most important dissolved gas, with average contents of c. 7 mol% N_2. Moreover, these fluids are commonly enriched in CH_4 (40% of the analyzed FI) and (in more than 50% of FI) also CO, averaging at 3 mol%. At El Hoyazo, a slight difference of T_{mCO_2} does occur between the two samples: this can be tentatively ascribed to the lower CH_4 contents of AVHZ8, as indicated by Raman results. Although in many Crd-hosted FI, CO_2 melting temperatures appear to be somewhat too low for the estimated compositions (see van den Kerkhof and Thiery, 1994, 2001), it should be recalled that Raman spectroscopy clearly shows the complex nature of these fluids, and it is possible that additional Raman inactive components (e.g., Ar; Touret, 1985), contributing to CO_2 triple point depression, may well be present in these inclusions.

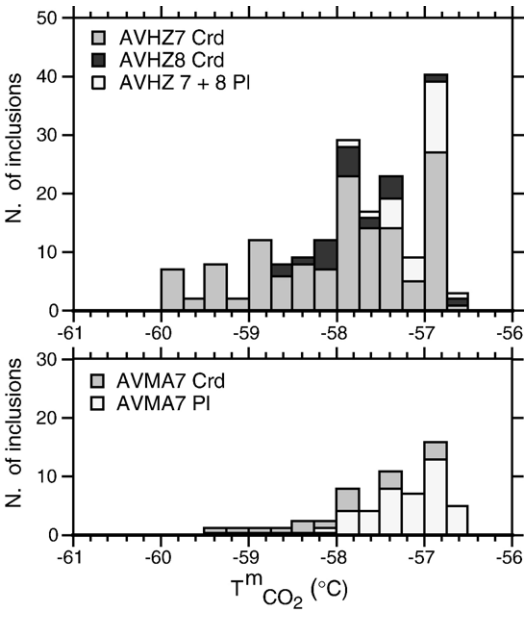

Fig. 6. Histograms of the melting temperature of the CO_2-rich solid.

Inclusions within El Hoyazo plagioclase are very rare (see Fig. 6), and systematically show higher T_{mCO_2} values, in agreement with the Raman finding of nearly pure CO_2 fluids with only minor contents (4–8 mol%) of N_2. Similarly, at Mazarrón, the T_{mCO_2} values correctly reflect an essentially pure carbonic phase, where some CH_4 was detected only within Pl-hosted FI. On the contrary, MT results (T_{mCO_2} = −57.0°/−59.5) clearly indicate that at Mazarrón, cordierites contain a fluid with higher contents of dissolved phases, compatible with Raman finding of higher CH_4 contents (10–22 mol %) along with some N_2.

Concerning the homogenization of the CO_2 phase, while homogenizations to the liquid are by far more common in sample AVHZ7 from El Hoyazo (see Table 3 and Fig. 7) in the other samples inclusions exhibit a variable microthermometric behaviour, where homogenizations both to the liquid or to the vapour were observed to occur within the same inclusion cluster or FIA. In these samples, most inclusions homogenize to the vapour. For AVHZ7 Crd-hosted inclusions, the same FI populations show a large range of homogenization temperatures, with T_{hCO_2} (L+V=L) ranging from +5 °C to +24 °C. Within the whole FI set, the lowest values (from +5 °C to +7.5 °C) were found in a cluster of 6 early monophase inclusions, while the majority of FI show higher homogenization temperatures, with two distinct peaks at +15 °C and +19 °C. In sample AVHZ8, T_{hCO_2} ranges from +15 °C to +24 °C in the vapour phase (L+V=V), while homogenizations to the liquid are very rare and scattered in temperature. On the whole, for homogenizations to the vapour, the temperature range basically overlaps with that of phase transitions to liquid (see Fig. 7). In all FI sets, Pl-hosted FI display T_{hCO_2} ranging from +15 °C to +25 °C, mostly to the vapour (Fig. 7).

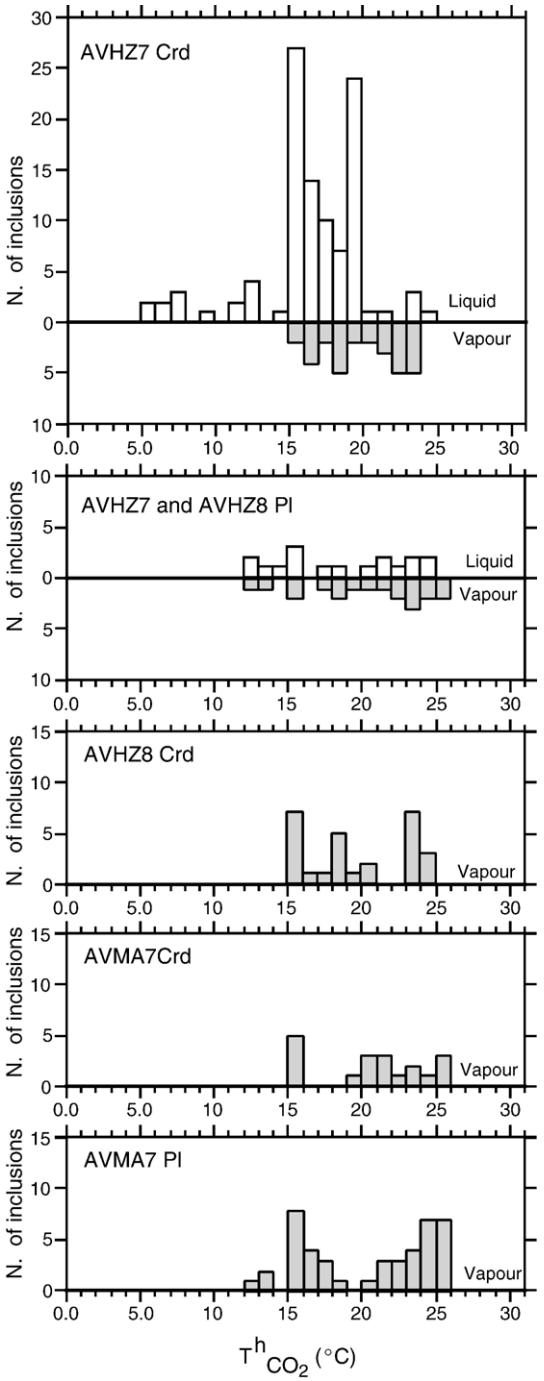

Fig. 7. Histograms of the homogenization temperature of CO_2.

5.4. Molar volume and isochore determinations

The chemical composition of all analyzed inclusions is defined by the C–O–H–N fluid system. Volumetric properties and isochores for representative inclusion compositions have been obtained by means of the software "FLUIDS" (Bakker, 2003). Molar volumes and densities in Table 3 were determined by the EOS of Thiery et al. (1994) and Soave (1972) for CO_2–N_2–CH_4 (±CO) mixtures, by introducing FI composition from Raman analyses and the homogenization conditions, T_{hCO_2}, from MT.

The isochores were then determined by using the EOS developed by Duan et al. (1992, 1996) for CO_2–CH_4–N_2–CO fluids, and by means of the EOS of Kerrick and Jacobs (1981) and Jacobs and Kerrick (1981) for CO_2–CH_4 binary fluids. As pressure correction for T_h, a temperature range between 800 and 900 °C, as derived from enclaves geothermometry, was considered for the trapping of both sample series. In detail, to calculate molar volumes and densities, we have considered an "average" fluid composition of 90 mol% CO_2, 7 mol% N_2, 3 mol% CO, as this is representative of the majority of Crd-hosted inclusion fluids, especially at El Hoyazo. As for El Hoyazo Pl-hosted inclusions the isochores were determined for a mean composition of 92 mol% CO_2–8 mol% N_2, whereas for Mazarrón the isochores were determined assuming a 95 mol% CO_2–5 mol% CH_4 average fluid composition.

As expected from MT data, fluid densities spread over a large interval, ranging from ~0.17 g cm^{-3}

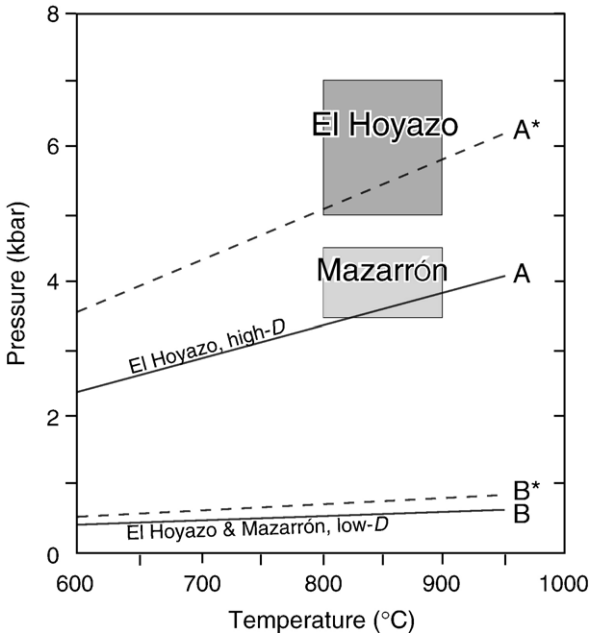

Fig. 8. *P–T* diagram comparing estimated *P–T* values of peak metamorphism and anatexis at El Hoyazo and Mazarrón (gray boxes), with representative calculated isochores for high-density FI of El Hoyazo (A) and low-density FI of both El Hoyazo and Mazarrón. Also reported are the displaced isochores (dashed, A* and B*) resulting after back-calculating the effect of leakage of 25 mol% H_2O.

(relative to the lowest homogenization temperatures to the vapour phase, T_{hCO_2}=15 °C), to a value of 0.82 g cm^{-3} for the lowest homogenization to the liquid phase of sample AVHZ 7 (T_{hCO_2}=5–7.5 °C). On a *P–T* grid, this would lead to maximum trapping pressures of ~4.0 kbar for the highest density fluids from El Hoyazo, and down to <1 kbar for the remaining Hoyazo lower density fluids and for all Mazarrón fluids (Fig. 8).

Because these values of pressure are very different from the inferred conditions of entrapment (see below), it is worth to consider the effects of a possible miscalculation of Crd-hosted FI components due to possible interferences between the Raman signal from structural fluids and that coming out from inclusion fluids (see above). Assuming the case of a pure CO_2 fluid rather than the detected mixture, the corresponding maximum density (for T_{hCO_2}=5.0 °C liq) would raise to ~0.9 g cm^{-3}, thereby placing trapping conditions about 0.5 kbar higher (i.e. around 5 kbar at *T*=900 °C). Although this value would fit with the lower limit of pressure estimates for El Hoyazo, yet in our dataset most FI would still maintain densities far below the values inferred from thermobarometry.

6. Discussion

The microstructural analysis indicates a simultaneous entrapment of an immiscible mixture of fluid and melt, strongly supports a primary origin for the studied FI and MI and, therefore, an entrapment during the thermal peak of anatexis, and does not show clear-cut evidence of post-entrapment reequilibration. These conclusions are at odds with calculated fluid densities, which provide isochores passing well below the pressures estimated from thermobarometric calculations by Cesare (2000) at El Hoyazo and by Álvarez-Valero (2004) at Mazarrón (Fig. 8).

A further problem arises from comparison of the chemical compositions of coexisting fluids and glasses, in particular H_2O concentrations. In fact, while glasses may contain appreciable quantities of H_2O (up to 3 wt mol%), fluids are H_2O-free. This is not consistent with the microstructural evidence of simultaneous entrapment (which strongly suggest equilibrium between fluid and melt), as a CO_2-rich fluid in equilibrium with a hydrated melt should contain detectable H_2O (Johannes and Holtz, 1996).

These apparent contradictions do not seem to be easily explained by decrepitation and leakage of the inclusions upon rapid decompression, because there is no straightforward microstructural evidence of these processes. Rejecting low-pressure leakage only from microstructural evidence may be considered too optimistic, as high-temperature annealing might wipe out the halos and trails of minute inclusions which are expected to form around large inclusions after decrepitation. However, even though decrepitation cannot be definitively ruled out, we can investigate the action of additional processes, occurring separately or, more likely, in close association for the decrease in the density of, and loss of H_2O from, the fluids. In the next section these processes are described and their relative importance assessed.

6.1. Causes of density decrease

Isochores have been calculated considering H_2O-free, C-bearing mixtures, in accordance with optical, MT, and Raman studies which did not detect any water. However, in rounded-shaped inclusions it is possible that small amounts of H_2O – less than 10 vol.% (Roedder, 1984; Crawford and Hollister, 1986) – forming an invisible thin film coating inclusion cavities, may be overlooked. Neglecting this hidden H_2O may produce significant errors when estimating the composition and density of FI, and might affect isochore calculations as well. For example, an addition of H_2O equivalent to 5 vol.%, would produce a displacement of calculated isochores of 0.4 kbar (at 800 °C) toward higher pressures for those inclusions with the highest density of El Hoyazo (d=0.82 g cm^{-3}). This effect vanishes with decreasing density in the fluid. Therefore, we conclude that undetected H_2O cannot be the main reason for a fictive depression of isochores from the inferred *P–T* anatectic conditions of trapping.

Since density can be diminished by both increasing the volume of the inclusion or diminishing the number of moles of fluid, a decrease in the density of fluids can be attained by several processes of both mechanical or chemical nature.

From a mechanical point of view, and in addition to inclusion decrepitation, inclusion volumes may expand by crystal-plastic deformation of the host phase during decompression at high temperature (i.e. during the uprise of enclaves within the host lava), as experimentally observed by Vityk and Bodnar (1995). There is no evidence of strain of hosts in the vicinity of inclusions, though this may have been erased by annealing at high temperature. In any case this process would explain only minor differences in calculated pressures of entrapment. An additional process which can have affected Crd-hosted inclusions is the phase transition between the HT hexagonal polymorph–indialite — and the orthorombic, denser, low *T* one. This phase transition may have favoured some volume increase of inclusions, but its effect should also be minor.

From a chemical perspective, density decrease can be explained by different processes which can take place both in open- and closed-system scenarios. Regarding open-systems, the main post-entrapment chemical modification leading to a density decrease is the leakage of components (Roedder, 1984; Kerrich, 1986). This process, detailed in the next section, is difficult to evaluate in the absence of evident decrepitation microstructures. However, and even in the absence of decrepitation, the current hosts phases – plagioclase and cordierite – are likely to be more favourable than others (e.g., quartz) for leakage of fluids from inclusions: the former for the presence of channels in its structure, the latter for the presence of twinning planes. These structures may favour the escape of fluids through the host's lattice. It is well known that CO_2 fluid inclusions constitute much stronger mechanical systems under strain/stress regimes with respect to aqueous ones, yet their leakage and density resetting is commonly observed. For instance, it is a very common phenomenon in mantle or crustal xenoliths and even volcanic rocks, where FI measurements frequently yield unrealistic low densities.

Densities can be diminished in a closed-system (i.e., without loss of mass) by at least two processes. One, which definitely took place in many inclusions, is the crystallization of denser daughter minerals, the other is fluid respeciation upon cooling. Daughter minerals are represented by calcite in Pl-hosted inclusions, and graphite in Crd-hosted inclusions. Formation of denser calcite by reaction of the less dense CO_2 of the fluid with the Ca of plagioclase results in diminishing the density of the fluid (Kleinefeld and Bakker, 2002). The same holds for graphite, which may precipitate by different respeciation reactions: some of them would form H_2O, (e.g., $CO_2+CH_4=2C+2H_2O$, Cesare, 1995) whereas others would not (e.g., $2CO=C+CO_2$). Because the size of daughter minerals is very small compared to that of inclusions, this process is likely to have produced only a minor effect on fluid densities. Respeciation on cooling, leading to a decrease in the number of moles in the system and, therefore, to a decrease in density, might also take place without formation of solids. An example of such a reaction involving the C–O–H species observed in inclusions could be: $2CO+2H_2=CO_2+CH_4$. Also this process, however, has a minor effect on fluid density.

It is apparent that, with the exclusion of extensive loss of components from the inclusions (see below), the mechanisms for the post-entrapment change of density described above are second-order phenomena which cannot account for the drastic density decrease inferred from microstructures and thermobarometry. The first-order process can be constrained by simultaneous consideration of the chemical relationships between fluid and associated melt inclusions.

6.2. Causes of chemical changes

When the two main compositional types of fluids are analyzed for consistency with inferred P–T conditions of entrapment, thermodynamic modelling of graphite-saturated fluids in the C–O–H system (Connolly and Cesare, 1993) shows that the fluids trapped at El Hoyazo (CH_4-free, CO-bearing, CO_2–N_2 mixtures) could be compatible with fluid speciation at high-temperature and low pressure, as supported by the presence of CO. On the contrary, the CH_4–CO_2 fluids in inclusions at Mazarrón are clearly metastable, since equilibrium would require the hydrogen component to be stored mostly in H_2O rather than in CH_4. Therefore, only the CH_4-free compositions of El Hoyazo might be representative of the primary fluids. However, also this conclusion appears to be untenable when compositions of coexisting glasses from melt inclusions are taken into account.

Table 1 shows that melt inclusions in cordierite from El Hoyazo may contain up to 3 wt.% H_2O. According to Johannes and Holtz (1996) these H_2O quantities require that the fluid in equilibrium with the glass had, in the pressure range 3–6 kbar, an H_2O mole fraction of up to 0.25. It follows that if the immiscible fluid and melt were trapped at equilibrium, inclusions must have leaked significant quantities of H_2O, either by diffusion through the channels of cordierite, or by any other reasonable mechanism, as summarized by Audetat and Gunther (1999).

We have modelled the effect of H_2O leakage by back-calculating the compositions and densities of representative inclusions from this study, when they are added with H_2O at constant volume, using for simplicity a pure CO_2 inclusion. It turns out that while addition of 25 mol % H_2O is able to raise of c. 2 kbar (from 3.5 to 5.5, at 850 °C) the isochores of denser fluid inclusions ($d=0.8$ g cm^{-3}), the same addition has minor to negligible effects for inclusions with densities <0.5.

We can conclude that the inclusions with the highest estimated densities from this study (c. 0.8) can represent the residuum after H_2O leakage, and that the additon of c. 25 mol% H_2O would make both their composition and density consistent with data from thermobarometry and melt inclusions. We can also conclude that none of the processes proposed here is able to reconcile the very low density ($d\approx 0.2$ g cm^{-3}) of most studied inclusions with their inferred P–T conditions of entrapment, unless

a major resetting of density at low-*P*, probably during lava uprise, has occurred.

The mobility of species in and out of FI is a long studied and debated issue, and it might be questioned why we have modelled the leakage of H_2O rather than of H_2, since this latter species has been experimentally proven to be very mobile (e.g., Morgan et al., 1993; Mavrogenes and Bodnar, 1994; Hall and Sterner, 1995). Since equilibrium considerations require H_2O as the leaked component, since H_2O is also considered quite mobile (Audetat and Gunther, 1999), and since we did not find evidence of H_2 diffusion out of inclusions, we prefer to model the process of leakage in terms of H_2O loss. Inspection of the C–O–H diagram of Fig. 5 shows that the two processes would have different consequences: while H_2O loss maintains the fluid along the carbon saturation curve keeping the ratio CO/CO_2 constant, diffusion of H_2 out of inclusions would make the fluid C-undersaturated, decreasing its CO fraction.

6.3. Constraints to temperature of anatexis

Estimates of temperatures of anatexis in the enclaves of El Hoyazo and Mazarrón rely on conventional thermometers such as garnet–biotite, garnet–cordierite, garnet–spinel–cordierite and ternary feldspars. At El Hoyazo, after a major event of melting at 850 ± 50 °C, 5–7 kbar (Cesare et al., 1997), further melting in some enclaves records peak temperatures of 900–950 °C, possibly at lower pressure of c. 5 kbar (Cesare, 2000). For Mazarrón, Álvarez-Valero (2004) calculated temperatures of 800–900 °C at c. 4 kbar. Under the assumptions that MI were trapped at the above pressure conditions, and that the estimated H_2O represent primary values, we can gain further constraints to the temperatures of entrapment from the composition of MI. Considering the minimum water contents of haplogranitic melts as a function of *P* and *T* (Johannes and Holtz, 1996), it is apparent that melts with $H_2O < 3$ wt.%, such as those of El Hoyazo inclusions, are stable at $T > 830$–850 °C in the 5–7 kbar region, and that temperature may be as high as 950 °C for inclusions with only 1 wt.% H_2O. At present we have no data on MI from Mazarrón enclaves. Therefore, thermometry based on H_2O contents of MI is an independent confirmation of estimates already available. One may speculate that the H_2O contents of glasses determined in this work are not the primary values, and that, as proposed for the FI, some H_2O may have diffused away also from MI. Although this hypothesis cannot be totally ruled out, two lines of observation make us consider it unlikely. The former is the absence of H_2O in the shrinkage bubbles of melt inclusions: if H_2O had diffused away, it should be also stored in these bubbles. The latter is the recent experimental evidence (Severs et al., 2005) that diffusive water loss is not a common phenomenon in MI.

6.4. Causes of fluid-melt immiscibility

F–M immiscibility indicates the coexistence at equilibrium of these two "fluid" phases, i.e., melt saturation with respect to the fluid. Fluid saturation is generally induced by decompression, owing to decreased solubility, or by crystallization of volatile-free solids. These processes are referred to as the "first- and second-boiling"of magma, (Burnham, 1979). In both cases, and in most studies, melt-fluid immiscibility is a retrograde (down-*P* and/or down-*T*) phenomenon, occurring during uprise and/or cooling of magmas (i.e., *after* their genesis). Conversely, immiscibility is very rarely documented as a *primary* feature during the prograde, up-*T* path leading to the generation of felsic anatectic melts.

Because: i) the studied samples are fragments of residual metasedimentary protoliths which underwent extensive melt extraction; ii) they were quenched through volcanic eruption and record high-temperature conditions in excess of 850 °C; iii) immiscible FI and MI appear to be primary in origin; iv) inclusions are trapped in hosts (cordierite and plagioclase) which are interpreted as products of peritectic reactions; v) solid inclusions in the hosts include biotite, garnet and sillimanite, which are interpreted as reactants in the same peritectic reactions; vi) the peraluminous granitic composition of the MI is consistent with partial melting of a metapelite, we conclude that the studied inclusions testify for fluid-melt immiscibility during the partial melting of the metapelitic enclaves. As such, they are one of the very rare natural examples of prograde immiscibility between granitic melt and CO_2-rich fluids. The CO_2-dominated character of the fluid is consistent with the high-*T* conditions of equilibration, and reflects the low solubility of this species in granitic melts, compared with that of H_2O (Tamic et al., 2001). While immiscibility requires that a carbonic fluid was present with the melt, it does not imply that the fluid was present before melting (Cesare et al., 2005).

6.5. Origin of CO_2 and N_2

The occurrence of CO_2 inclusions within mantle xenoliths has been documented in many localities within different geodynamic contexts, sometimes even in association with melt inclusions (e.g. Roedder, 1994 and references therein; Frezzotti et al., 1994), supporting

the idea of a common and widespread occurrence of carbonic fluids within the upper mantle and in mantle-derived magmas. The same applies to a certain extent to high-grade metamorphic crustal rocks, where the presence of CO_2 in granulites, and its coexistence with an anatectic granitic melt is a well known and long debated issue of lower crustal petrology (e.g., Farquhar and Chacko, 1991; Clemens, 1993). The origin of CO_2 in metapelitic granulites has been recently reviewed by Cesare et al. (2005): along with other possibilities, they discussed also the hypothesis that, in graphitic rocks, CO_2 may be originated during the incongruent, dehydration melting of Fe^{3+}-bearing biotite. This model, which predicts the oxidation of the metasedimentary graphite by simultaneous reduction of the Fe^{3+}, implies an internal derivation of the carbonic fluid, consequential to the partial melting process. Since at both El Hoyazo and Mazarrón the enclaves are graphitic (Cesare and Maineri, 1999; Cesare et al., 2003b), we infer that such an origin of CO_2 may be envisaged also in the present study.

An internally-derived origin can be proposed also for the N_2 component of the fluid inclusions. It is well known that NH_4^+ groups may substitute for K^+ in the structure of a number of silicates, notably micas (e.g. Sadofsky and Bebout, 2000). Therefore, the melting of NH_4^+-bearing biotite can release nitrogen in the fluid (Kreulen and Schuiling, 1982; Moine et al., 1994). The data of Cesare et al. (2003c), reporting up to 900 ppm NH_4 in biotites from the enclaves of El Hoyazo, support this hypothesis. In addition, nitrogen may also be retained in the heavy residues during the maturation of organic matter, and may be liberated during progressive graphitization or during graphite consumption (Norman and Palin, 1982; Haendal et al., 1986).

7. Concluding remarks

Although the observed microstructures do not reveal any clear-cut evidence of post-entrapment modifications, we have concluded that FI must have undergone significant changes, both chemically and/or volumetrically, in order to be compatible with their estimated *P–T* conditions of trapping. The chemical changes must have involved leakage of significant quantities of H_2O, but this alone cannot explain the very low densities (c. 0.2 g cm^{-3}) of most FI: further loss of the carbonic component, or significant volume expansion, possibly helped by crystal plasticity during decompression at HT, are required.

Even though it should be expected that FI are unable to maintain an isochoric closed system during fast isothermal decompression of >4 kbar, as in the present case study, it appears as if the type of host mineral – plagioclase and cordierite – may have enhanced post-entrapment resetting. It may be possible that more rigid and chemically refractory hosts, such as garnet, could preserve inclusions from late modifications, but unfortunately in the studied enclaves garnet was a reactant phase during melting and immiscible entrapment.

Despite an incompleteness of information on the precise nature of fluids in equilibrium with the anatectic granitic melt, this study is probably unique in providing data on fluid-melt chemical relationships during anatexis of graphitic metapelites and genesis of S-type granites. Being based on an atypical natural case study, this work can help integrate experimental and field-based research on deep crustal petrogenetic processes such as the granite–granulite connexion (e.g., Clemens, 1990).

Acknowledgements

We acknowledge the financial support of Università di Padova (Fondi Progetti Ricerca 2002) and Consiglio Nazionale delle Ricerche. This work has also been made possible thanks to the support of 01-LECEMA22F "WESTMED — Imaging the western Mediterranean margins: a key target to understand the interaction between deep and shallow processes" Project by the European Science Foundation under the EUROCORES Programme EUROMARGINS, through contract No. ERAS-CT-2003-980409 of the European Commission, DG. We wish to thank F. Degli Antonini for the help with Raman analyses, A. Álvarez-Valero and M.T. Gómez-Pugnaire for the assistance during sampling, J. Connolly, M.L. Frezzotti, F. Holtz, D. London, M. Satish Kumar and J. Touret for their helpful discussions, T. Andersen and J.M. Huizenga for their reviews. M.L Frezzotti and A.M. Van den Kerkhof are thanked for their careful editorial handling.

References

Acosta-Vigil, A., London, D., Morgan VI, G.B., Dewers, T.A., 2003. Solubility of excess alumina in hydrous granitic melts in equilibrium with peraluminous minerals at 700–800 °C and 200 MPa, and applications of the aluminum saturation index. Contrib. Mineral. Petrol. 146, 100–119.

Acosta-Vigil, A., Cesare, B., London, D., Morgan, G.B., VI, 2007-this issue. Microstructures and composition of melt inclusions in a crustal anatectic environment: the metapelitic enclaves within El Hoyazo dacites, SE Spain Chem. Geol. doi:10.1016/j.chemgeo.2006.07.014.

Aines, R.D., Rossman, G.R., 1984. The high temperature behaviour of water and carbon dioxide in cordierite and beryl. Am. Mineral. 69, 319–327.

Álvarez-Valero, A., 2004. Petrographic and thermodynamic study of the partial melting of restitic xenoliths from the Neogene Volcanic Province of SE Spain. PhD Thesis, Università di Padova.

Álvarez-Valero, A.M., Cesare, B., Kriegsman, L., 2005. Formation of elliptical garnets in a metapelitic enclave by melt-assisted dissolution and reprecipitation. J. Metamorph. Geol. 23, 65–74.

Andersen, T., Neumann, E.R., 2001. Fluid inclusions in mantle xenoliths. Lithos 55, 301–320.

Armbruster, T., 1985. Ar, N_2 and CO_2 in the structural cavities of cordierite, an optical and X-ray single crystal study. Phys. Chem. Miner. 12, 233–245.

Armbruster, T., Bloss, F.D., 1982. Orientation and effects of channel H_2O and CO_2 in cordierite. Am. Mineral. 67, 284–291.

Audetat, A., Gunther, D., 1999. Mobility and H_2O loss from fluid inclusions in natural quartz crystals. Contrib. Mineral. Petrol. 137 (1–2), 1–14.

Bakker, R.J., 2003. Package FLUIDS 1. Computer programs for analysis of fluid inclusion data and for modelling bulk fluid properties. Chem. Geol. 194, 3–23.

Burke, E.A.J., 1994. Raman microspectrometry of fluid inclusions: the daily practice. In: De Vivo, B., Frezzotti, M.L. (Eds.), Fluid Inclusions in Minerals: Methods and Application. IMA Short Course, Virginia Polytechnic Institute and State Univ. Press, Blacksburg, VA, pp. 25–44.

Burke, E.A.J., 2001. Raman microspectrometry of fluid inclusions. Lithos 55, 139–158.

Burnham, C.W., 1979. Magmas and hydrothermal fluids, In: Barnes, H.L. (Ed.), Geochemistry of Hydrothermal Ore Deposits, 2nd ed. Wiley, New York, pp. 71–136.

Cesare, B., 1995. Graphite precipitation within C–O–H fluid inclusions: closed-system chemical and density changes, and thermobarometric implications. Contrib. Mineral Petrol. 122, 25–33.

Cesare, B., 2000. Incongruent melting of biotite to spinel in a quartz-free restite at El Joyazo (SE Spain): textures and reaction characterization. Contrib. Mineral Petrol. 139, 273–284.

Cesare, B., Maineri, C., 1999. Fluid-present anatexis of metapelites at El Joyazo (SE Spain): constraints from Raman spectroscopy of graphite. Contrib. Mineral. Petrol. 35, 41–52.

Cesare, B., Gomez-Pugnaire, M.T., 2001. Crustal melting in the Alborán domain: constraints from the xenoliths of the Neogene Volcanic Province. Phys. Chem. Earth, Part A 26 (4–5), 255–260.

Cesare, B., Salvioli Mariani, E., Venturelli, G., 1997. Crustal anatexis and melt extraction in the restitic xenoliths at El Hoyazo (SE Spain). Min. Mag. 61, 15–27.

Cesare, B., Gomez-Pugnaire, M.T., Rubatto, D., 2003a. Residence time of S-type anatectic magmas beneath the Neogene Volcanic Province of SE Spain: a zircon and monazite SHRIMP study. Contrib. Mineral. Petrol. 146, 28–43.

Cesare, B., Marchesi, C., Hermann, J., Gomez-Pugnaire, MT., 2003b. Primary melt inclusions in andalusite from anatectic graphitic metapelites: implications for the position of the Al_2SiO_5 triple point. Geology 31, 573–576.

Cesare, B., Cruciani, G., Russo, U., 2003c. Hydrogen deficiency in Ti-rich biotite from anatectic metapelites (El Joyazo— SE Spain): crystal-chemical aspects and implications for high-temperature petrogenesis. Am. Mineral. 88, 583–595.

Cesare, B., Meli, S., Nodari, L., Russo, U., 2005. Fe^{3+} reduction during biotite melting in graphitic metapelites: another origin of CO_2 in granulites. Contrib. Mineral Petrol. 149, 129–140.

Clemens, J.D., 1990. The granulite–granite connexion. In: Vielzeuf, D., Vidal, P. (Eds.), Granulites and Crustal Differentiation. Kluwer Academic Publishers, Dordrecht, pp. 25–36.

Clemens, J.D., 1993. Experimental evidence against CO_2-promoted deep crustal melting. Nature 363, 336–338.

Clemens, J.D, Vielzeuf, D., 1987. Constraints on melting and magma production in the crust. Earth Planet. Sci. Lett. 86, 287–306.

Connolly, J., Cesare, B., 1993. C–O–H–S fluid composition and oxygen fugacity in graphitic metapelites. J. Metamorph. Geol. 11, 379–388.

Crawford, M.L., Hollister, L.S., 1986. Metamorphic fluids: the evidence from fluid inclusion. In: Walther, J.V. (Ed.), Physical Geochemistry, vol. 5, pp. 1–35.

Damon, P.E., Kulp, J.L., 1958. Excess helium and argon in beryl and other minerals. Am. Mineral. 43, 433–459.

De Vivo, B., Frezzotti, M.L., 1994. Evidence for magmatic immiscibility in Italian subvolcanic systems. In: De Vivo, B., Frezzotti, M.L. (Eds.), Fluid Inclusions in Minerals: Methods and Application. IMA Short Course, Virginia Polytechnic Institute and State Univ. Press, Blacksburg, VA, pp. 209–215.

Duan, Z., Moller, N., Weare, J.H., 1992. Molecular dynamics simulation pf PVT properties of geological fluids and a general equation of state of nonpolar and weakly polar gases up to 2000 K and 20,000 bar. Geochim. Cosmochim. Acta 56, 3839–3845.

Duan, Z., Moller, N., Weare, J.H., 1996. A general equation of state for supercritical fluid mixture and molecular dynamics simulation of mixture PVTX properties. Geochim. Cosmochim. Acta 60, 1209–1216.

Ebadi, A., Johannes, W., 1991. Beginning of melting and composition of first melts in the system Qz–Ab–Or–H_2O–CO_2. Contrib. Mineral. Petrol. 106, 286–295.

Farquhar, J., Chacko, T., 1991. Isotopic evidence for involvement of CO_2-bearing magmas in granulite formation. Nature 354, 60–63.

Frezzotti, M.L., Touret, J.L.R., Lustenhouwer, W., Neumann, E.R., 1994. Melt and fluid inclusions in dunite xenoliths from La Gomera, Canary Islands: tracking the mantle metasomatic fluids. Eur. J. Mineral. 6, 805–817.

Goldman, D.S., Rossman, G.R., Dollase, W.A., 1977. Channel constituents in cordierite. Am. Mineral. 62, 1144–1157.

Goldstein, R.H., Reynolds, T.J., 1994. Systematics of fluid inclusions in diagenetic minerals. S.E.P.M. Short Course 31 199 pp.

Haendal, D., Muhle, K., Nitzsche, H.M., Steihl, G., Wand, U., 1986. Isotopic variation of the fixed nitrogen in metamorphic rocks. Geochim. Cosmochim. Acta 50, 749–758.

Hall, D.L., Sterner, M., 1995. Experimental diffusion of hydrogen into synthetic fluid inclusions in quartz. J. Metamorph. Geol. 13, 345–355.

Herms, P., Schenk, V., 1992. Fluid inclusions in granulite-facies metapelites of Hercynian ancient lower crust of the Serre, Calabria, Southern Italy. Contrib. Mineral. Petrol. 112, 393–404.

Holloway, J.R., 1976. Fluids in the evolution of granitic magmas: consequences of finite CO_2 solubility. GSA Bull. 87, 1513–1518.

Jacobs, G.K., Kerrick, D.M., 1981. Methane: an equation of state with applications to ternary system H_2O–CO_2–CH_4. Geochim. Cosmochim. Acta 45, 607–614.

Johannes, W., Holtz, F., 1996. Petrogenesis and Experimental Petrology of Granitic Rocks. Springer Verlag. 335 pp.

Kalt, A., 2000. Cordierite channel volatiles as evidence for dehydration melting: an example from high-temperature metapelites of the Bayerische Wald (Variscan belt, Germany). Eur. J. Mineral. 12, 987–998.

Kerrich, R., 1986. Fluid infiltration into fault zone: chemical, isotopic and mechanical effects. Pure Appl. Geophys. 124, 225–268.

Kerrick, D.M., Jacobs, G.K., 1981. A modified Redlich–Kwong equation for H_2O–CO_2 mixtures at elevated pressures and temperatures. Am. J. Sci. 281, 735–767.

Khomenko, V.M., Langer, K., 2000. Aliphatic hydrocarbons in structural channels of cordierite: a first evidence from polarized single-crystal IR-absorption spectroscopy. Am. Mineral. 84, 1181–1185.

Kleinefeld, B., Bakker, R.J., 2002. Fluid inclusions as micro-chemical systems: evidence and modelling of fluid–host interactions in plagioclase. J. Metamorph. Geol. 20, 845–858.

Kolesov, B.A., Geiger, C.A., 2000. Cordierite II: the role of CO_2 and H_2O. Am. Mineral. 85, 1265–1274.

Kretz, R., 1983. Symbols for rock-forming minerals. Am. Mineral. 68, 277–279.

Kreulen, R., Schuiling, R.D., 1982. N_2–CH_4–CO_2 fluids during formation of the dome de l'Agout, France. Geochim. Cosmochim. Acta 46, 193–203.

Kurepin, V.A., Malyuk, G.A., Kalinichenko, A.M., Utochkin, D.V., 1986. Volatile components in cordierite from Berdichev granulites (Ukrainian Shield). Mineral. Z. 8 (2), 70–82 (In Russian).

Le Breton, N., Thompson, A.B., 1988. Fluid-absent (dehydration) melting of biotite in metapelites in the early stages of crustal anatexis. Contrib. Mineral Petrol. 99, 226–237.

Lowenstern, J.B., 1995. Applications of silicate-melt inclusions to the study of magmatic volatiles. Magmas, fluids, and ore deposits. In: Thompson, J.F.H. (Ed.), MAC Short Course, vol. 23. Victoria, British Columbia, pp. 71–100.

Lowenstern, J.B., 2003. Melt inclusions come of age: volatiles, volcanoes, and Sorby's legacy. In: De Vivo, B., Bodnar, R.J. (Eds.), Melt Inclusions in Volcanic Systems: Methods, Applications and Problems. Developments in Volcanology, vol. 5. Elsevier Press, Amsterdam, pp. 1–22.

Mavrogenes, J.A., Bodnar, R.J., 1994. Hydrogen movement into and out of fluid inclusions in quartz: experimental evidence and geological implications. Geochim. Cosmochim. Acta 58, 141–148.

McCreery, R.L., 2000. Raman Spectroscopy for Chemical Analysis. Wiley - Interscience, New York. Chapter 10.

Moine, B., Guillot, C., Gibert, F., 1994. Controls of the composition of nitrogen-rich fluids originating from reaction with graphite and ammonium-bearing biotite. Geochim. Cosmochim. Acta 58, 5503–5523.

Morgan VI, G.B., London, D., 1996. Optimizing the electron microprobe analysis of hydrous alkali aluminosilicate glasses. Am. Mineral. 81, 1176–1185.

Morgan VI, G.B., Chou, I.M., Pasteris, J.D., 1993. Speciation in experimental C–O–H fluids produced by the therma dissociation of oxalic acid dihydrate. Geochim. Cosmochim. Acta 56, 281–294.

Mottana, A.R., Fusi, A., Potenza, B.B., Liborio, G., Crespi, R., 1983. Hydrocarbon-bearing cordierite from Cervio–Dolico road tunnel (Como, Italy). Neues Jahrb. Mineral. Abh. 148, 186–199.

Norman, D.I., Palin, J.M., 1982. Volatiles in phyllosilicate minerals. Nature 296, 551–553.

Patiño Douce, A.E., Johnston, A.D., 1991. Phase equilibria and melt productivity in the pelitic system: implications for the origin of peraluminous granitoids. Contrib. Mineral. Petrol. 107, 202–218.

Pouchou, J.L., Pichoir, F., 1985. "PAP" $\phi(\rho z)$ correction procedure for improved quantitative microanalysis. In: Armstrong, J.T. (Ed.), Microbeam Analysis. San Francisco Press, San Francisco, pp. 104–106.

Roedder, E., 1965. Liquid CO inclusions in olivine-bearing nodules and phenocrysts from basalts. Am. Mineral. 50, 1746–1782.

Roedder, E., 1984. Fluid inclusions. Rev. Miner. 12.

Roedder, E., 1992. Fluid inclusion evidence for immiscibility in magmatic differentiation. Geochim. Cosmochim. Acta 56, 5–20.

Roedder, E., 1994. Fluid inclusions evidence of mantle fluids. In: De Vivo, B., Frezzotti, M.L. (Eds.), Fluid Inclusions in Minerals: Methods and Application. IMA Short Course, Virginia Polytechnic Institute and State Univ. Pres, Blacksburg, VA, pp. 283–296.

Roedder, E., Coombs, V.D., 1967. Immiscibility in granitic melts, indicated by fluid inclusions in ejected granitic blocks of Ascencion Islands. J. Petrol. 8, 417–451.

Sadofsky, S.J., Bebout, G.E., 2000. Ammonium partitioning and nitrogen-isotope fractionation among coexisting micas during high-temperature fluid–rock interactions; examples from the New England Appalachians. Geochim. Cosmochim. Acta 64, 2835–2849.

Severs, M., Azbej, T., Thomas, J., Mandeville, C., Bodnar, R.J., 2005. Do melt inclusions record water contents of the original melt? Ecrofi XVIII, Siena.

Soave, G., 1972. Equilibrium constants from a Modified Redlich–Kwong equation of state. Chem. Eng. Sci. 27, 1197–1203.

Tamic, N., Behrens, H., Holtz, F., 2001. The solubility of H_2O and CO_2 in rhyolitic melts in equilibrium with a mixed CO_2–H_2O fluid phase. Chem. Geol. 174, 333–347.

Thiery, R., Vidal, J., Dubessy, J., 1994. Phase equilibria modelling applied to fluid inclusions: liquid-vapor equilibria and calculation of the molar volume in CO_2–CH_4–N_2 system. Geochim. Cosmochim. Acta 58, 1073–1082.

Touret, J.L.R., 1971. Le faciès granulite en Norvège méridionale. II Les inclusions fluides. Lithos 4, 423–436.

Touret, J.L.R., 1981. Fluid inclusions in high grade metamorphic rocks. In: Hollister, L.S., Crawford, M.L. (Eds.), Short Course in Fluid Inclusions: Applications to Petrology. Min. Assoc. Canada, Calgary, pp. 182–208.

Touret, J.L.R., 1985. Fluid regime in Southern Norway: the record of fluid inclusions. In: Tobi, A.C., Touret, J.L.R. (Eds.), The Deep Proterozoic Crust in the North Atlantic Provinces. Reidel, Dordrecht, pp. 517–549.

van den Kerkhof, A.M., Thiéry, R., 1994. Phase density calculation in the CO_2–CH_4–N_2 system. In: De Vivo, B., Frezzotti, M.L. (Eds.), Fluid Inclusion in Minerals: Methods and Applications. Short Course of the Working Group (IMA) "Inclusions in Minerals", pp. 171–190.

van den Kerkhof, A.M., Thiéry, R., 2001. Carbonic inclusions. In: Andersen, T., Frezzotti, M.L., Burke, E.A.J. (Eds.), Fluid Inclusions: Phase Relationships–Methods–Applications. Special Volume in Honour of Jacques Touret. Lithos, vol. 55, pp. 49–68.

van den Kerkhof, A.M., Touret, J.L.R., Maijer, C., Jansen, J.B.H., 1991. Retrograde methane-dominated fluid inclusions from high-temperature granulites of Rogaland, southwestern Norway. Geochim. Cosmochim. Acta 55, 2533–2544.

Vielzeuf, D., Holloway, J.R., 1988. Experimental determination of the fluid-absent melting relations in the pelitic system. Consequences for crustal differentiation. Contrib. Mineral. Petrol. 98, 257–276.

Vityk, M.O., Bodnar, R.J., 1995. Textural evolution of synthetic fluid inclusion in quartz during reequilibration, with application to tectonic reconstruction. Contrib. Mineral Petrol. 121, 309–323.

Winkler, H.G.F., 1974. Petrogenesis of Metamorphic Rocks, 3rd ed. Springer-Verlag, New York.

Winslow, D.M., Erickson, C.J., Tracy, R.J., Bodnar, R.J., 1991. Evidence for nitrogen-rich metamorphic fluids in the Central Maine Terrane of south-central Massachusetts. Geol. Soc. Am. Abstr. Program 23, 335.

Zeck, H.P., 1970. An erupted migmatite from Cerro de Hoyazo, SE Spain. Contrib. Mineral. Petrol. 26, 225–246.